Structural aspects of two-stage dimerization in an ionic C_{60} complex with bis(benzene)chromium: $Cr(C_6H_6)_2 \cdot C_{60} \cdot C_6H_4Cl_2$

Dmitri V. Konarev,*[a,b] Salavat S. Khasanov,[a,c] Andrey Y. Kovalevsky,[d] Gunzi Saito,*[a] Akihiro Otsuka[e] and Rimma N. Lyubovskaya[b]

Received 13th March 2006, Accepted 25th April 2006
First published as an Advance Article on the web 4th May 2006
DOI: 10.1039/b603685f

Single crystals of the ionic C_{60} complex with bis(benzene)chromium: $\{Cr^I(C_6H_6)_2^{\bullet+}\} \cdot (C_{60}^{\bullet-}) \cdot C_6H_4Cl_2$ (**1**) were obtained. The crystal structure of **1** shows the presence of monomeric $C_{60}^{\bullet-}$ radical anions at 250 K and the formation of single-bonded $(C_{60}^-)_2$ dimers at 90 K. The dimerization is realized in two types of the $C_{60}^{\bullet-}$ pairs with different interfullerene center-to-center distances of 10.052 and 10.279 Å arranged in zigzag chains along the *a*-direction. As a result, two symmetrically independent $(C_{60}^-)_2$ dimers found in **1** at 90 K have different environments, intercage C–C bond lengths and C_{60}^- center-to-center distances. Such differences should provide different thermal stability of these dimers and result in the appearance of two stages at the dimerization. Indeed, according to SQUID measurements, the magnetic moment of **1** decreases stepwise at the dimerization in two temperature ranges at 240–200 and 200–160 K.

Introduction

Interest to ionic fullerene compounds is evoked by their promising physical properties[1–3] and a large variety of dimeric and polymeric structures formed by negatively charged fullerenes.[4–10] Up to now single-bonded $(C_{60}^-)_2$ (Fig. 1) and $(C_{70}^-)_2$ dimers, $(C_{60}^-)_x$, $(C_{60}^{3-})_x$, $(C_{70}^{2-})_x$ and $(C_{70}^{3-})_x$ linear polymers bonded by one and two single bonds and two-dimensional $(C_{60}^{4-})_x$ polymers bonded by four single bonds have been found.[4–10] Dimerization is realized as a reversible structural transition beginning at 140–250 K and results in abrupt changes in magnetic properties of the complexes, namely, paramagnetic–diamagnetic transitions or a decrease of the magnetic moment.[5–8,11,12] Dimerization was found in different ionic complexes and salts of C_{60}: metastable $M \cdot C_{60}$ phases (M = K, Rb, and Cs);[13–15] $Cr(C_6H_5Me)_2 \cdot C_{60}$ ($Cr(C_6H_5Me)_2$: bis(toluene)chromium) at 250 K;[5] $Cp^*{}_2Cr \cdot C_{60} \cdot (C_6H_4Cl_2)_2$ ($Cp^*{}_2Cr$: decamethylchromocene) at 220–200 K;[7,11] polycrystalline $Cr(C_6H_6)_2 \cdot C_{60} \cdot (C_6H_4Cl_2)_{0.7}$ and $Cr(C_6H_6)_2 \cdot C_{60} \cdot C_6H_5CN$ ($Cr(C_6H_6)_2$: bis(benzene)chromium) at 160–240 and above 250 K, respectively;[7] $Cp_2Co \cdot C_{60} \cdot C_6H_4Cl_2$ (Cp_2Co: cobaltocene) at 250–350 K;[7] multi-component $(Cs)_2 \cdot (C_{60})_2 \cdot CTV \cdot (DMF)_6$ (CTV: cyclotriveratrylene) at 140–220 K;[8] $Cr(C_6H_6)_2 \cdot C_{60} \cdot [Pd(dbdtc)_2]_{0.5}$ ($Pd(dbdtc)_2$: palladium(II) dibenzyldithiocarbamate) at 130–150 K;[12] and $Cr(C_6H_5–C_6H_5)_2 \cdot C_{60}$ ($Cr(C_6H_5–C_6H_5)_2$: bis(diphenyl)chromium.[16] In spite of a large variety of compounds, which show dimerization, the dimerization process has not been studied well. In most of the complexes either dimerization was investigated only by X-ray powder diffraction or the crystal structure of only one phase (dimeric or monomeric) was determined. There is only one complex, $Cp^*{}_2Cr \cdot C_{60} \cdot (C_6H_4Cl_2)_2$, whose crystal structure was studied both for monomeric and dimeric phases by X-ray diffraction on a single crystal. That allowed one to study the molecular structure of the $(C_{60}^-)_2$ dimer and understand the dimerization mechanism in this complex.[7,11]

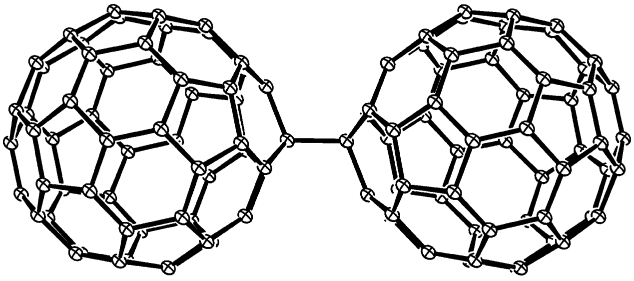

Fig. 1 Molecular structure of a single-bonded $(C_{60}^-)_2$ dimer.

In the present work single crystals of another ionic fullerene complex with bis(benzene)chromium: $Cr(C_6H_6)_2 \cdot C_{60} \cdot C_6H_4Cl_2$ (**1**) were obtained. This complex is a second example in which dimerization was observed and the crystal structure was determined both for monomeric and dimeric phases at 250 and 90 K, respectively. Structural aspects of the dimerization were studied in detail clarifying the peculiarities of the magnetic behavior of **1**.

Results and discussion

Previously the polycrystalline ionic $Cr(C_6H_6)_2 \cdot C_{60} \cdot (C_6H_4Cl_2)_{0.7}$ complex was obtained and characterized by elemental analysis, IR-, UV-vis-NIR, EPR spectroscopies and SQUID technique.[7] The reversible decrease of the magnetic moment of the complex in the 240–160 K range is attributed to the formation of diamagnetic

---

[a] *Division of Chemistry, Graduate School of Science, Kyoto University, Sakyo-ku, Kyoto, 606-8502, Japan. E-mail: saito@kuchem.kyoto-u.ac.jp; Fax: +81-75-753-40-35*
[b] *Institute of Problems of Chemical Physics RAS, Chernogolovka, Russia. E-mail: konarev@icp.ac.ru; Fax: +007-496- 515-54-20*
[c] *Institute of Solid State Physics RAS, Chernogolovka, Moscow Region, 142432, Russia*
[d] *State University of New York at Buffalo, Buffalo, New York, 14214, USA*
[e] *Research Center for Low Temperature and Materials Sciences, Kyoto University, Sakyo-ku, Kyoto, 606-8502, Japan*

single-bonded $(C_{60}^{-})_2$ dimers. However, it was impossible to understand the peculiarities of dimerization in $Cr(C_6H_6)_2\cdot C_{60}\cdot(C_6H_4Cl_2)_{0.7}$ since its crystal structure was not determined. Now single crystals of this complex have been obtained by the two month diffusion of hexane into a *o*-dichlorobenzene solution containing C_{60} and two molar equivalents of $Cr(C_6H_6)_2$. The composition of the complex was refined in accordance with the X-ray diffraction data as $Cr(C_6H_6)_2\cdot C_{60}\cdot C_6H_4Cl_2$ (**1**).

IR- and UV-vis-NIR spectra of **1** indicate its ionic ground state: $\{Cr^I(C_6H_6)_2^{\bullet+}\}\cdot(C_{60}^{\bullet-})\cdot C_6H_4Cl_2$. The shift of the $F_{1u}(4)$ band from 1429 to 1390 cm^{-1} and the inversion of the intensities of the $F_{1u}(1)$ and $F_{1u}(2)$ modes at 525 and 574 cm^{-1}, respectively, as well as the appearance of bands in the NIR-range at 936 and 1078 nm are characteristic of $C_{60}^{\bullet-}$.[17] The bands at 418 and 460 cm^{-1} are sensitive to the charged state of $Cr(C_6H_6)_2$ and have the same positions as in the spectrum of $(Cr^I(C_6H_6)_2^{\bullet+})(I^-)$[18] indicating the formation of $Cr^I(C_6H_6)_2^{\bullet+}$ radical cations.

The data of magnetic measurements for **1** are shown in Fig. 2. The magnetic moment of **1** is $2.45\mu_B$ at 300 K and slightly decreases with temperature down to 240 K. This value is close to that calculated for a system containing two $S = 1/2$ spins indicating that both $Cr^I(C_6H_6)_2^{\bullet+}$ and $C_{60}^{\bullet-}$ with 1/2 spin state contribute to the magnetic susceptibility above 240 K. The magnetic moment reversibly decreases below 240 K down to $1.73\mu_B$ at 160 K (Fig. 2). Since the value of the magnetic moment (μ_{eff}) for a non-interacting $S = 1/2$ system is also 1.73 μ_B, below 160 K only one 1/2 spin contributes to the magnetic susceptibility. Dimerization is accompanied by changes in the EPR spectrum of **1**. The EPR signal with $g = 1.9913$ at 285 K is intermediate between those characteristic of $Cr^I(C_6H_6)_2^{\bullet+}$ ($g = 1.9860$[19]) and $C_{60}^{\bullet-}$ ($g = 1.9996$–2.0000[17]) showing strong exchange coupling between these ion-radicals. On cooling **1** in the 240–160 K range the *g*-factor shifts to 1.9860, which is characteristic of non-interacting paramagnetic $Cr^I(C_6H_6)_2^{\bullet+}$.[19] Therefore, one 1/2 spin per formula unit retained below 160 K is localized on $Cr^I(C_6H_6)_2^{\bullet+}$, whereas $C_{60}^{\bullet-}$ spins disappear due to bond formation in the diamagnetic single-bonded $(C_{60}^{-})_2$ dimers. The magnetic transition in **1** has two peculiarities. It is unusually broad (calc. about 80 K) with two well-resolved steps in the temperature dependence curve of magnetic moment (Fig. 2). The boundary between the steps lies at about 200 K, when approximately 50% of dimers is formed. Such behavior can be explained if two dimers with different thermal stability are present in the sample. The temperature dependences of the magnetic moment upon cooling and heating indicate the reversibility of dimerization and reproduce the two stages of the dimerization. It should be noted that in previously described ionic complexes of C_{60} the dimerization is conventionally a one-stage process and occurs in narrower temperature ranges.[5,7,11,12]

Magnetic data indicate that the dimeric phase is formed in **1** below 160 K, whereas a monomeric phase should exist above 240 K. Two temperatures (90 and 250 K) were thus chosen for X-ray diffraction experiments. The crystal structure at 250 K contains orientationally disordered monomeric $C_{60}^{\bullet-}$ radical anions, which rotate almost freely. Due to small sizes of $Cr^I(C_6H_6)_2^{\bullet+}$ radical cations and $C_6H_4Cl_2$ molecules, the $C_{60}^{\bullet-}$ radical anions are packed close to each other in a complicated 3D packing with each $C_{60}^{\bullet-}$ having five neighbors. Two $C_{60}^{\bullet-}$ are located in zigzag chains passing along the *a*-direction with alternating interfullerene center-to-center distances of 10.052 and 10.279 Å. Fig. 3 shows views on the chains (a) and along the chains (b), with the chains marked by dashed lines. The former distance is close to that in pure C_{60} crystal at 153 K (the center-to-center distance is 9.94 Å),[20] whereas the latter is noticeably longer than the van der Waals radius of C_{60} (10.18 Å), indicating the absence of interfullerene C–C contacts in these pairs. Two other $C_{60}^{\bullet-}$ are located in the *bc*-plane at an equal distance of 10.085 Å (Fig. 3(b)). The neighbor with the shortest interfullerene center-to-center distance of 10.013 Å is located approximately in the *c*-direction (Fig. 3(b)). Therefore, there are five directions along which $C_{60}^{\bullet-}$ radical anions

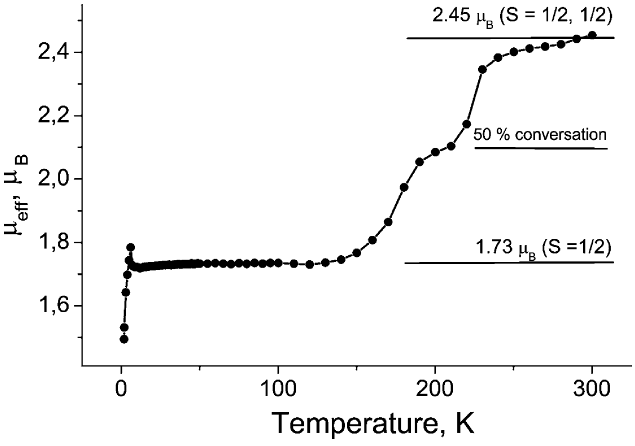

Fig. 2 Temperature dependence of the magnetic moment of **1** in the 1.9–300 K range. The behaviour is reversible.

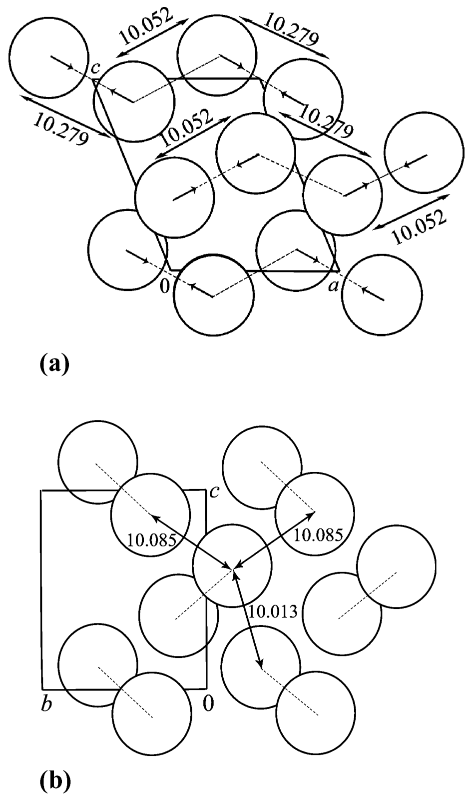

Fig. 3 Packing of $C_{60}^{\bullet-}$ radical anions (circles) in monomeric phase of **1** at 250 K. Views along the *b*- (a) and *a*-axes (b) are shown. Dashed lines show the zigzag chains arranged along the *a*-direction in which the dimerization is realized. Arrows show the direction of the dimerization.

can dimerize in **1** with four different center-to-center distances ranging from 10.013 to 10.279 Å.

Dimerization results in a structural transition from a monoclinic lattice with $P2_1/c$ symmetry to a triclinic lattice with lower $P\bar{1}$ symmetry. In contrast to $Cp^*{}_2Cr{\cdot}C_{60}{\cdot}(C_6H_4Cl_2)_2$,[7] no doubling of the unit cell was observed. The cell size remains almost unchanged in the *a*-direction (15.604(4) and 15.601(1) Å). However, it slightly expands in the *c*-direction (from 19.461(5) to 19.746(2) Å) and noticeably shrinks in the *b*-direction (from 15.313(4) to 14.662(1) Å). Dimerization is realized in two kinds of $C_{60}^{\bullet-}$ pairs with different interfullerene center-to-center distances of 10.052 and 10.279 Å arranged in zigzag chains along the *a*-direction (Fig. 3(a)). As a result, two symmetrically independent dimers are formed in **1** at 90 K. These dimers have different environments formed by $Cr^{I}(C_6H_6)_2^{\bullet+}$ and $C_6H_4Cl_2$ moieties, and have slightly different intercage C–C bond lengths (1.585(5) and 1.595(5) Å) and interfullerene center-to-center distances (9.262 and 9.271 Å). While only one type of zigzag chains are arranged in the *a*-direction in the monomeric phase (Fig. 3(a) and (b)), two types of such chains are formed in the dimeric phase. The interfullerene center-to-center distances in these chains are 9.262 and 9.271 Å inside the dimers, and 10.205 and 10.598 Å between the C_{60}^{-} anions from neighboring dimers (Fig. 4(a) and (b)). The $C_{60}^{\bullet-}$ pairs of the monomeric phase with a shorter interfullerene center-to-center distance of 10.052 Å afford dimers with a shorter intercage C–C bond length (1.585(5) Å) and shorter interfullerene center-to-center distances in the chains (9.262 and 10.205 Å). The main reason for the appearance of different dimers in **1** is the initial structural differentiation of the $C_{60}^{\bullet-}$ pairs in which the dimerization is realized. On the contrary, $C_6H_4Cl_2$ molecules and bulky $Cp^*{}_2Cr^+$ cations isolate zigzag chains from $C_{60}^{\bullet-}$ radical anions in $Cp^*{}_2Cr{\cdot}C_{60}{\cdot}(C_6H_4Cl_2)_2$ with uniform interfullerene center-to-center distances of 10.1 Å. As a result, the $C_{60}^{\bullet-}$ radical anions have only a single route for the dimerization. The center-to-center distances in the zigzag chain of the dimeric phase is 9.28 Å inside the dimers and 9.91 Å between C_{60}^{-} from neighboring dimers.[7]

It was shown that the temperature of the beginning of dimerization in the studied ionic C_{60} complexes varies essentially from 140 up to >250 K. Most probably, such variety originates from different interfullerene center-to-center distances in the monomeric phases of the complexes that results in different interfullerene C–C contacts, and different environments of $C_{60}^{\bullet-}$ from counter cations and solvent molecules.[8] Structural and magnetic data obtained for **1** allow us to suppose that different single-bonded $(C_{60}^{-})_2$ dimers with different thermal stabilities can form even in a single complex. The dimerization temperatures for such dimers are shifted relative to each other (the shift is about 40 K), which provide two-stage dimerization in **1** at 240–200 and 200–160 K. We can assume that in the first stage (240–200 K) the dimerization is realized in the $C_{60}^{\bullet-}$ pairs with the 10.052 Å distance, whereas the $C_{60}^{\bullet-}$ pairs with 10.279 Å distance are excluded from the dimerization because of large distances between $C_{60}^{\bullet-}$. Most probably, the dimerization in the first stage shrinks the lattice and makes remaining nondimerized $C_{60}^{\bullet-}$ approach closer to each other (as compared with the 10.279 Å distance) providing the possibility for the dimerization in the second stage below 200 K.

It is unusual that the *a*-direction (with 10.052 and 10.279 Å interfullerene distances) is more preferable for the dimerization in spite of that interfullerene distances in other directions are noticeably shorter (10.013 and 10.085 Å). Most probably, the main reason for this is the difference in the environment of $C_{60}^{\bullet-}$. Only $C_6H_4Cl_2$ molecules are inserted between the fullerene anions in the zigzag chains passing in the *a*-direction, which can be shifted during the dimerization allowing the formation of interfullerene σ-bonds, whereas bulkier $Cr^{I}(C_6H_6)_2^{\bullet+}$ radical cations separate $C_{60}^{\bullet-}$ and prevent their dimerization in other directions (Fig. 5(a) and (b)).

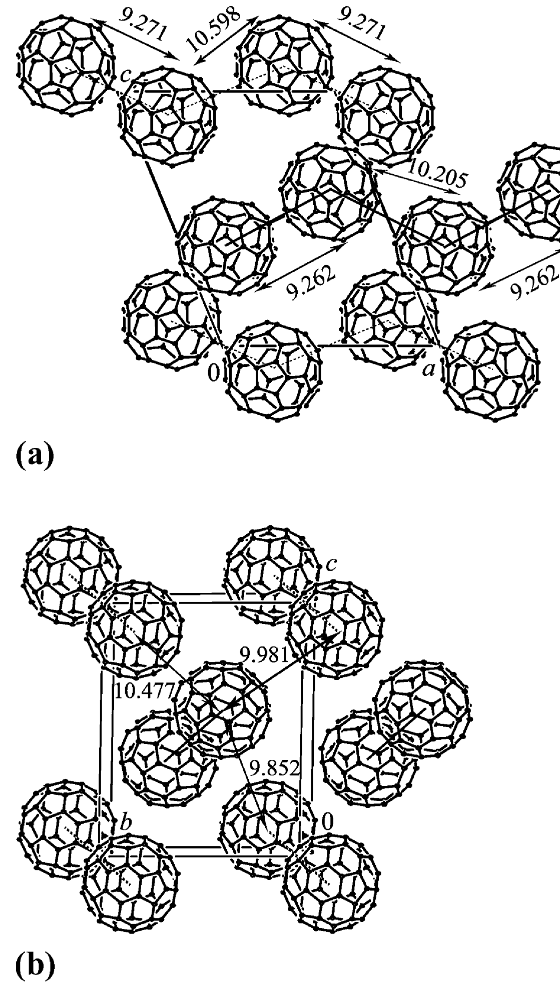

Fig. 4 Packing the $(C_{60}^{-})_2$ dimers in **1** at 90 K. Views along the *b*- (a) and *a*-axes (b) are shown. Only one of two orientations of the $(C_{60}^{-})_2$ dimers is depicted. Dashed and thin lines show the two types of zigzag chains, in which the dimerization is realized.

Conclusion

The C_{60} complex with bis(benzene)chromium, $Cr(C_6H_6)_2{\cdot}C_{60}{\cdot}C_6H_4Cl_2$ (**1**), was obtained as single crystals and the crystal structure of monomeric and dimeric phases was studied at 90 and 250 K. The dimerization is realized in two types of $C_{60}^{\bullet-}$ pairs with different interfullerene center-to-center distances of 10.052 and 10.279 Å arranged in zigzag chains along the *a*-direction. This provides the formation of two symmetrically independent $(C_{60}^{-})_2$ dimers at 90 K, which differ in their environment, the intercage C–C bond length (1.585(5) and 1.595(5) Å) and the interfullerene center-to-center distances (9.262 and 9.271 Å). We suppose that

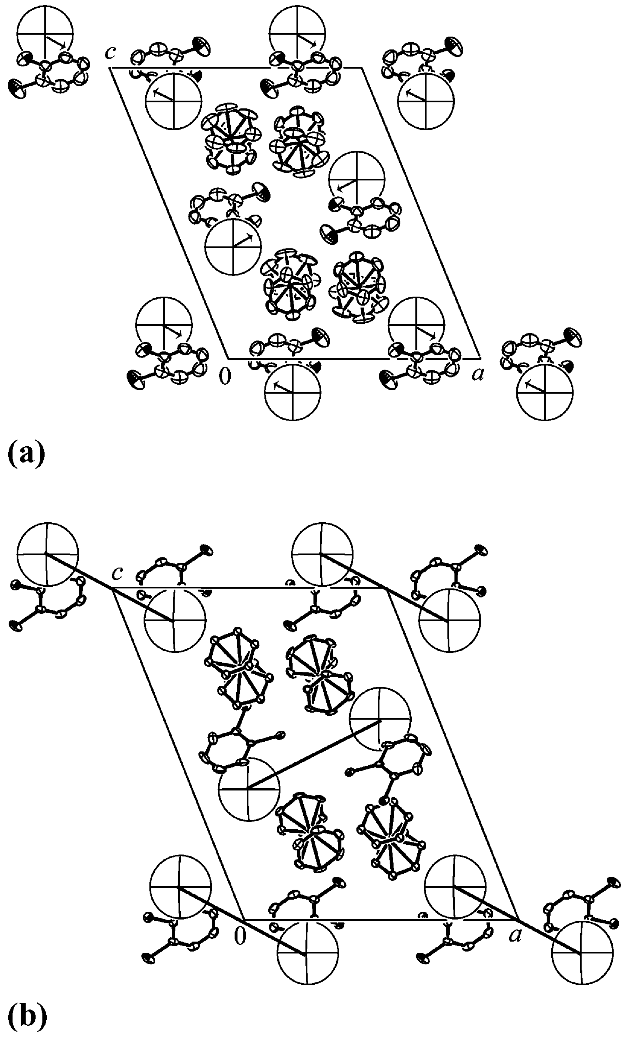

Fig. 5 The changes in the arrangement of $\mathrm{Cr^I(C_6H_6)_2}^{\bullet+}$ radical cations and $C_6H_4Cl_2$ molecules at the dimerization: (a) the monomeric phase at 250 K and (b) the dimeric phase at 90 K. C_{60}^- anions are shown by centroids. Only one orientation with major occupation is depicted for disordered $\mathrm{Cr^I(C_6H_6)_2}^{\bullet+}$ and $C_6H_4Cl_2$ moieties.

these structural differences affect the thermal stability of the dimers and result in the appearance of two-stage dimerization as derived from magnetic measurements. We can conclude that the dimerization in **1** is governed by two main factors. The initial distances between $C_{60}^{\bullet-}$ in the monomeric phase affect the dimerization temperature, whereas the environment of $C_{60}^{\bullet-}$ from $\mathrm{Cr^I(C_6H_6)_2}^{\bullet+}$ radical cations and solvent $C_6H_4Cl_2$ molecules defines the direction of the dimerization.

Experimental

Materials

$\mathrm{Cr(C_6H_6)_2}$ was purchased from Strem Chemicals, and C_{60} of 99.98% purity was used from MTR Ltd. Hexane was distilled over Na/benzophenone and *o*-dichlorobenzene ($C_6H_4Cl_2$) was distilled over CaH_2 under reduced pressure in an argon atmosphere. For the synthesis of air-sensitive **1**, solvents were degassed and stored in a glove-box. All manipulations for the synthesis of the crystals were carried out in a MBraun 150B-G glove box with controlled atmosphere and a content of H_2O and O_2 less than 1 ppm. The crystals were stored in a glove-box and were sealed in 2 mm quartz tubes for EPR and SQUID measurements at 10^{-5} Torr. KBr pellets for IR and UV-visible-NIR measurements were prepared in a glove box.

Synthesis

$\mathrm{Cr(C_6H_6)_2 \cdot C_{60} \cdot C_6H_4Cl_2}$ (**1**) was obtained by a slow diffusion of hexane (20 mL) in an *o*-dichlorobenzene solution (20 mL) containing C_{60} (0.035 mmol, 25 mg) and 2 mol equivalents of $\mathrm{Cr(C_6H_6)_2}$ (0.070 mmol, 14.5 mg) in a glass tube of 1.5 cm diameter and 50 mL volume with a ground glass plug. After 2 months, crystals of **1** were formed on the wall of the tube. The solvent was decanted from the precipitated crystals, which were washed with hexane to yield black prisms in 80% yield.

The composition of the complex was determined by elemental analysis[7] and was corrected according to X-ray diffraction data for a single crystal. IR Spectrum of **1**: 418s, 460m, 525m, 574s, 657w, 748s, 784m, 813w, 835w, 972w, 1002m, 1030m, 1122m, 1143w, 1181w, 1263w, 1390s, 1430m, 1453m cm^{-1}. NIR spectrum: 265, 341, 936, 1078 nm.

General

FT-IR spectra were measured in KBr pellets with a Perkin-Elmer 1000 Series spectrometer (400–7800 cm^{-1}). UV-visible-NIR spectra were measured on a Shimadzu-3100 spectrometer in the 220–1600 nm range. A Quantum Design MPMS-XL SQUID magnetometer was used to measure static susceptibilities at 100 mT magnetic field in heating and cooling modes (1.9–300 K). EPR spectra were recorded from 285 K down to 4 K with a JEOL JES-TE 200 X-band ESR spectrometer.

X-Ray crystal structure determination

Crystal data for 1 at 250(2) K. $\mathrm{C_{78}H_{16}Cl_2Cr}$, $M_r = 1075.81$ g mol^{-1}, black prisms, monoclinic, $P2_1/c$, $a = 15.604(4)$, $b = 15.313(4)$, $c = 19.461(5)$ Å, $\beta = 112.225(8)°$, $V = 4305(2)$ Å^3, $Z = 4$, $D_c = 1.660$ g cm^{-3}, $\mu = 0.450$ mm^{-1}, $F(000) = 2168$, max. $2\theta_{max} = 57.14°$. In total, 67618 reflections were measured, 10934 of which were independent. The least-squares refinement on F^2 was done to R_1 $[F > 2\sigma(F)] = 0.0456$ for 8238 observed reflections, $wR_2 = 0.1311$ (all data), $R_1 = 0.0622$ for all 10934 observed reflections with 852 parameters and 2174 restraints; final GOF = 1.037. CCDC reference number 600437.

Crystal data for 1 at 90(2) K. $\mathrm{C_{78}H_{16}Cl_2Cr}$, $M_r = 1075.81$ g mol^{-1}, black prisms, triclinic, $P\bar{1}$, $a = 15.6010(13)$, $b = 14.6619(12)$, $c = 19.7463(16)$ Å, $\alpha = 90.973(3)$, $\beta = 112.455(2)$, $\gamma = 86.799(3)°$, $V = 4167.8(6)$ Å^3, $Z = 4$, $D_c = 1.715$ g cm^{-3}, $\mu = 0.465$ mm^{-1}, $F(000) = 2168$, max. $2\theta_{max} = 55.3°$. In total, 58042 reflections were measured, 18432 of which were independent. The least-squares refinement on F^2 was done to R_1 $[F > 2\sigma(F)] = 0.0611$ for 12675 observed reflections, $wR_2 = 0.1783$ (all data), $R_1 = 0.0943$ for all 18432 observed reflections with 1398 parameters and 2174 restraints; final GOF = 1.011. CCDC reference number 600438.

The X-ray diffraction data were collected at 90 and 250 K on a Bruker SMART1000 CCD diffractometer equipped with a rotating anode (Mo-Kα radiation, $\lambda = 0.71073$ Å). The data were collected by the rotation method with a 0.3° frame width (ω scan). The data collection nominally covered half of the reciprocal space by a combination of six ω scans (600 frames in each set), with different ϕ angles. Reflection intensities were integrated using the SAINT program.[21]

The solution and refinement of the structures were performed with SHELXTL program package.[22] The structures were refined by full-matrix least squares against F^2 for all data. Non-hydrogen atoms were refined anisotropically, and isotropically for fullerene molecule at 90 K. Hydrogen atoms were assigned geometrically.

For crystallographic data in CIF or other electronic format see DOI: 10.1039/b603685f

Disorder in the crystal structure of 1 at 250 and 90 K.

At 250 K. Fullerene molecules in the structure of **1** rotate almost freely. Disordered fullerene molecules were approximated with 180 carbon atoms with 1/3 occupancy, assigned to electron density peaks after using the direct method and consequent Fourier syntheses. Atomic coordinates and anisotropic thermal parameters for fullerene atoms were refined by a SHELXL conjugate-gradient least square procedure in the early stages and full-matrix least square procedure in the final refinement, with thermal parameters fixed. $Cr^I(C_6H_6)_2^{\bullet+}$ radical cations are disordered between two orientations with 0.51/0.49 occupancies related by their rotation by 20° about the axis passing through the centers of two benzene rings and chromium atom. $C_6H_4Cl_2$ molecules are also disordered between two orientations with 0.61/0.39 occupancies.

At 90 K. The $(C_{60}^-)_2$ dimers are fixed in two orientations linked to each other by the rotation about the longer axis of the dumb-bell $(C_{60}^-)_2$ with an angle of 106 and 120° for the two symmetrically independent dimers. The occupancy factors are 0.5/0.5 for both dimers. There are two symmetrically independent $Cr^I(C_6H_6)_2^{\bullet+}$ radical cations. One radical cation showed no indication of disorder, while the other one is disordered into two positions with 0.58/0.42 occupancies. One $C_6H_4Cl_2$ site is ordered, while the other is disordered.

Acknowledgements

The work was supported by Grant-in-Aid Scientific Research from the Ministry of Education, Culture, Sports, Science and Technology, Japan (152005019, COE programs), the Russian Science Support Foundation, INTAS YSF 05-109-4653 and RFBR grant N 06-03-32824.

References

1 M. J. Rosseinsky, *J. Mater. Chem.*, 1995, **5**, 1497.
2 B. Gotschy, *Fullerene Sci. Technol.*, 1996, **4**, 677.
3 D. V. Konarev and R. N. Lyubovskaya, *Russ. Chem. Rev.*, 1999, **68**, 19.
4 K. Prassides, in *The Physics of Fullerene-based and Fullerene-related materials*, ed. W. Andreoni, Kluwer Academic Publishers, Dordrecht, 2000, p. 175.
5 A. Hönnerscheid, L. Wüllen, M. Jansen, J. Rahmer and M. Mehring, *J. Chem. Phys.*, 2001, **115**, 7161.
6 D. V. Konarev, S. S. Khasanov, I. I. Vorontsov, G. Saito, Yu. A. Antipin, A. Otsuka and R. N. Lyubovskaya, *Chem. Commun.*, 2002, 2548.
7 D. V. Konarev, S. S. Khasanov, G. Saito, A. Otsuka, Y. Yoshida and R. N. Lyubovskaya, *J. Am. Chem. Soc.*, 2003, **125**, 10074.
8 D. V. Konarev, S. S. Khasanov, G. Saito and R. N. Lyubovskaya, *Recent Res. Develop. Chem.*, 2004, **2**, 105.
9 H. Brumm, E. Peters and M. Jansen, *Angew. Chem., Int. Ed.*, 2001, **40**, 2069.
10 M. Panthöfer, U. Wedig, H. Brumm and M. Jansen, *Solid State Sci.*, 2004, **6**, 619.
11 D. V. Konarev, S. S. Khasanov, A. Otsuka and G. Saito, *J. Am. Chem. Soc.*, 2002, **124**, 8520.
12 D. V. Konarev, A. Yu. Kovalevsky, A. Otsuka, G. Saito and R. N. Lyubovskaya, *Inorg. Chem.*, 2005, **44**, 9547.
13 Q. Zhu, D. E. Cox and J. E. Fischer, *Phys. Rev. B: Condens. Matter*, 1995, **51**, 3966.
14 G. Oszlányi, G. Bortel, G. Faigel, M. Tegze, L. Grárásy, S. Pekker, P. W. Stephens, G. Bendele, R. Dinnebier, G. Mihály, A. Jánossy, O. Chauvet and L. Forró, *Phys. Rev. B: Condens. Matter*, 1995, **51**, 12228.
15 M. Kosaka, K. Tanigaki, T. Tanaka, T. Atake, A. Lappas and T. Prassides, *Phys. Rev. B: Condens. Matter*, 1995, **51**, 12018.
16 S. Yu. Ketkov, G. A. Domrachev, A. M. Ob'edkov, A. Yu. Vasil'kov, L. P. Yur'eva and C. P. Mehner, *Russ. Chem. Bull.*, 2004, **53**, 1932.
17 C. A. Reed and R. D. Bolskar, *Chem. Rev.*, 2000, **100**, 1075.
18 H. P. Fritz, W. Lüttke, H. Stammreich and R. Forneris, *Chem. Ber.*, 1959, **92**, 3246.
19 C. Elschenbroich, E. Bilger and J. Koch, *J. Am. Chem. Soc.*, 1984, **106**, 4297.
20 H.-B. Burgi, E. Blanc, D. Schwarzenbach, S. Liu, Y.-J. Lu, M. M. Kappers and J. A. Ibers, *Angew. Chem., Int. Ed. Engl.*, 1992, **31**, 640.
21 *SMART and SAINT, Area Detector Control and Integration Software, Ver. 6.01.* Bruker. Analytical X-ray Systems, Madison, WI, 1999.
22 *SHELXTL, An Integrated System for Solving, Refining and Displaying Crystal Structures from Diffraction Data, Ver. 5.10.* Bruker Analytical X-ray Systems, Madison, WI, USA, 1997.